A new technique for MR elastography of the supraspinatus muscle: a gradient-echo type multi-echo sequence

Daiki Ito [a], Tomokazu Numano [a], Kazuyuki Mizuhara [b], Koichi Takamoto [c], Takaaki Onishi [a], Hisao Nishijo [c, d]

[a] Department of Radiological Science, Graduate School of Human Health Science, Tokyo Metropolitan University
7-2-10, Higashiogu, Arakawa-ku, Tokyo, Japan
TEL +81-3-3819-1211
FAX +81-3-3819-1406
e-mail: t-numano@tmu.ac.jp

[b] Department of Mechanical Engineering, Tokyo Denki University

[c] Department of Neurophysiotherapy, and [d] System Emotional Science, Graduate School of Medicine and Pharmaceutical Sciences, University of Toyama

Abstract

Magnetic resonance elastography (MRE) can measure tissue stiffness quantitatively and noninvasively. Supraspinatus muscle injury is a significant problem among throwing athletes. The purpose of this study was to develop an MRE technique for application to the supraspinatus-muscle by using a conventional magnetic resonance imaging (MRI). MRE acquisitions were performed with a gradient-echo type multi-echo MR sequence at 100 Hz pneumatic vibration. A custom-designed vibration pad was used as a pneumatic transducer in order to adapt to individual shoulder shapes. In a gradient-echo type multi-echo MR sequence, without motion encoding gradient (MEG) that synchronizes with vibrations, bipolar readout gradient lobes achieved a similar function to MEG (MEG-like effect). In other words, a dedicated MRE sequence (built-in MEG) is not always necessary for MRE. In this study, 7 healthy volunteers underwent MRE. We investigated the effects of direction of the MEG-like effect and selected imaging planes on the patterns of wave propagation (wave image). The results indicated that wave images showed clear wave propagation on a condition that the direction of the MEG-like effect was nearly perpendicular to the long axis of the supraspinatus-muscle, and that the imaging plane was superior to the proximal supraspinatus-muscle. This limited condition might be ascribed to specific features of fibers in the supraspinatus–muscle and wave reflection from the boundaries of the supraspinous fossa. The mean stiffness of the supraspinatus muscle was 10.6 ± 3.18 kPa. Our results demonstrated that using MRE, our method can be applied to the supraspinatus muscle by using conventional MRI.

Keywords: MR elastography; Shoulder; Supraspinatus; Muscle; Muscle fiber; Stiffnes

1. Introduction

Palpation and biopsies remain the fundamental clinical tools to diagnose abnormal stiffness changes in soft tissue. Palpation is a non-invasive technique; however, it is subjective, and detecting stiffness changes is impossible in all tissues, for example, deep or small tissues. Biopsies are an invasive technique, and may impose a high burden on patients. With that in mind, elastography was developed

using ultrasound [1,2] and magnetic resonance imaging (MRI) [3]. These techniques are noninvasive, and provide quantitative information on tissue stiffness.

Elastography using MRI, i.e., MR elastography (MRE), uses harmonic mechanical excitation to measure mechanical properties such as shear modulus (or stiffness) of tissues [3,4]. MRE allows measurement of mechanical properties of both superficial and deep tissues only if vibrations reach these tissues. In MRE, imaging pulse sequence synchronizes with the harmonic mechanical excitation. Tissue displacements due to vibrations are encoded into an MR phase image (wave image) by using bipolar gradient lobes (motion-encoding gradient: MEG). Recoded wave images are converted into the shear stiffness value by a variety of processing techniques [5]. In recent years, MRE has been increasingly used to measure the mechanical properties of tissues in vivo, such as the brain [4-6], breast [4,5,7], liver [4,8,9], prostate [10,11], and skeletal muscles [4,5,12-15].

Mechanical properties of skeletal muscles are strongly affected by various pathologic and physiologic states. Skeletal muscle MRE can provide quantitative information on the mechanical properties of pathologic and physiologic states, for example, contractile [4,5,12,13], diseased and damaged states [16,17]. Previous studies have reported that shear wave displacements were induced primarily perpendicular to the muscle fibers [5,18] because of the anisotropy of the muscle. Moreover, other previous studies have demonstrated that shear wave velocity depends on the direction of wave propagation to the muscle fibers [19,20]. MRE allows visualization of tissue displacements due to vibrations in the MEG direction. Therefore, selection of the MEG direction is a very important parameter in skeletal muscle MRE.

Shoulder injuries are significant problems among throwing athletes (those who play baseball, volleyball, tennis, etc.). In particular, rotator cuff injuries often occur. Rotator cuff tears usually initiate at the anterosuperior portion of the supraspinatus muscle and extend posteriorly [21]. After a tear of the supraspinatus tendon, the musculotendinous unit refracts permanently, undergoes the muscle atrophies and fatty infiltration, and loses elasticity [22]. Hence, the evaluating the stiffness of the supraspinatus muscle could assist the diagnosis and for examination of the effect of treatments relating to rotator cuff tears. However,-it is difficult to palpate the supraspinatus muscle because it is difficult to determine their anatomic location superficially. In the rotator cuff, palpating the subscapular muscle is also difficult. Many previous studies have assessed an increase in T2 relaxation time (T2) as an

indicator of muscle damages after exercise [23-25]. Yanagisawa et al. [26] also reported that an increase in T2 in the supraspinatus muscle was greater than that in the subscapular muscle after baseball pitching. Hence, the supraspinatus muscle is likely to be more susceptible to damages compared to the subscapular muscle in throwing athletes. For these reasons, stiffness measurement of the supraspinatus muscle using MRE would be required for clinical diagnosis.

The purpose of this study was to develop an MRE technique to be applied to the supraspinatus muscle. We used a conventional gradient-echo type multi-echo MR sequence developed by Numano et al. [15] in order to conduct an MRE of the supraspinatus muscle using a conventional MRI. Andrea et al. [27] measured the stiffness of the supraspinatus muscle using ultrasound elastography. However, it is difficult to measure the absolute values of stiffness in this method. As far as we know, only one previous study evaluated stiffness of the shoulder muscle using MRE [14], in which only the infraspinatus muscle was evaluated. This is the first study to apply MRE to the supraspinatus muscle. However, there are 3 problems with the application of MRE to the supraspinatus muscle. First, the supraspinatus muscle has a morphologically complex structure and is one of the uni-circumpennate muscles with an intramuscular tendon. Second, the supraspinatus muscle is located in the supraspinous fossa. Therefore, the propagating wave in the supraspinatus muscle is distorted by reflection from the boundary between the SPP muscle and the supraspinous fossa. Third, shoulder shape differs greatly across individuals. It is difficult for the driver of excitation to be placed in the same position regardless of shoulder shapes. To resolve these problems, we developed a new MRE technique that could be applied to the supraspinatus muscle.

2. Materials and methods

2.1. Participants

Seven healthy volunteers (7 men, age range: 20-42 years) were enrolled in this MRE study. All volunteer studies were performed after obtaining informed consent from the participants and after receiving approval from our institutional ethnic review board.

2.2. Experimental setup

All MRI and MRE experiments were performed on a clinical MR imager (Achieva 3.0T; Philips Healthcare, Best, The Netherlands) while using a shoulder coil with the subject in the supine position. We instructed the volunteers to relax during imaging, but did not instruct them to take specific body positions, for example, flexing and stretching the elbow joint. A self-made waveform generation system (LabVIEW, USB-6221; National Instruments, TX, USA) was used to generate the vibration waveform. In order to synchronize the vibration with TR, the transistor-transistor logic (TTL) signal from the MRI system (RF pulse power amplifier) was used as a trigger to start the vibration. This system was capable of generating sinusoidal waveforms with arbitrary frequencies and phases. In this MRE system, the vibration phase offset was controlled by the waveform generator, giving continuous (steady state) vibrations throughout the whole acquisition (each imaging period). A power amplifier (XTi 1000; Crown, IN USA) and a pneumatic pressure generator (Subwoofer TIT320C-4 12”; Dayton Audio, OH, USA) were used to supply vibrations to a vibration pad (Fig. 1a) through a hose. The vibration pad was designed by using a three-dimensional (3D) printer (3Dtouch; 3D System, SC, USA) in order to adapt to individual shoulder shapes.

Fig. 1b-d shows an MRE setup. The vibration pad was placed over the trapezius muscle on the proximal side of the supraspinatus muscle and was secured using Velcro straps and an auxiliary tool which was designed by using a 3D printer. In addition, a silicon sheet was placed between the vibration pad and the skin on the trapezius muscle. The silicon sheet plays an important role as a substitute for the vibration membrane and prevents air from leaking through the interstices between the vibration pad and the skin on the trapezius muscle.

2.3. MR elastography and anatomical MRI

MRE acquisitions were performed with a gradient-echo type multi-echo MR sequence and axial images of the supraspinatus muscle were obtained. In a gradient-echo type multi-echo MR sequence, multiple symmetrical gradient-echoes were acquired by the symmetrical bipolar readout gradient lobes. If those gradient lobes are synchronized with vibrations, they have a similar function to MEG (MEG-

like effect). This synchronization can be easily achieved by adjusting the period of bipolar readout gradient lobes and the gap between the first and next echo (δTE) of a multi-echo sequence. If the δTE is synchronized with the vibration frequency, the readout gradient lobes have maximum MEG-like effect. Moreover, the later generated echo has greater MEG-like effect (1st echo < 2nd echo < 3rd echo, etc.). A gradient-echo type multi-echo MR sequence has 2 benefits. First, multiple gradient-echoes are useful to reduce the acquisition time of MRI or MRE. Second, a multi-echo MR sequence acquires images with different weightings and/or TEs and is used to obtain various images without increasing the acquisition time. However, it is impossible to detect the vibration perpendicular to the imaging plane because the motion-encoding direction depends on the readout gradient direction. Further details have been described in the study by Numano et al".

We conducted MRE of the supraspinatus muscle at 100 Hz vibration, and it was synchronized with 5 ms of δTE. The 100 Hz vibration frequency was chosen as a tradeoff between penetration depth and resolution of the stiffness of the supraspinatus muscle. The MR phase images (wave images) were recoeded with the following parameters: 256×256 acquisition matrix, 8 number of averages, 2 SENSE reduction factor, 20° flip angle, 170-180 mm field of view, 5 mm slice thickness, 2.3 ms 1st TE, 7.3 ms 2nd TE, 12.3 ms 3rd TE, 20 ms repetition time, and 80 s total acquisition time (4 vibration phase offsets). In the case of the first echo data, wave images represented unclear wave propagation in the supraspinatus muscle because MEG-like effect is not enough to visualize wave propagation. In the case of the second and third echo data, wave images represented clear wave propagation in the supraspinatus muscle because MEG-like effect is enough to visualize wave propagation. The third echo data were affected by transverse relaxation compared with that of the second echo data. Hence, this study used the second echo data. Moreover, in this method, the MEG-like effect, and its direction were determined by the readout gradient intensity and the readout direction, respectively. For investigating changes in wave images by the direction of the MEG-like effect, the wave images were obtained for each angle of rotation of the readout direction with regard to the long axis of the supraspinatus muscle (readout-angle) from 0-150°, with a 30° step (Fig. 2a). The readout-angle rotation was achieved by rotating the imaging plane (Fig. 2b). The readout gradient intensity (MEG-like effect) was kept constant by maintaining the field of view and acquisition matrix constant in each readout-angle. Moreover, the MEG-like effect can resolve vector components of the MEG-like effect

perpendicular (perpendicular-MEG-like effect) and parallel (parallel-MEG-like effect) to the long axis of the supraspinatus muscle (Fig. 2c).

A series of oblique coronal and sagittal proton-density-weighted images of the supraspinatus muscle were acquired with a Turbo Spin Echo MRI sequence. The acquired data were used as a reference for muscle shape to accurately obtain the wave images. Mashhour et al. [13] reported that the pattern of the wave image changed by the angle of the selected imaging plane in the thigh muscles. In this study, the wave images were obtained for 4 imaging planes (Fig. 3). Each imaging plane was determined by the following procedure: First, the baseline was determined based on 2 thickest lines of the intramuscular tendon on an oblique coronal image. Second, imaging planes were set parallel to the baseline on the oblique coronal image. Finally, imaging planes were set at the superior (imaging plane: IP #1 and IP #3) or inferior portion (IP #2 and IP #4) on the proximal side of the supraspinatus muscle on an oblique sagittal image.

2.4. Image processing and data analysis

All wave images were processed by a phase unwrapping and a Gaussian spatial filter (MRE/Wave, MAYO CLINIC) after extracting the supraspinatus muscle from raw data. The region of interest (ROI) was set along the inner surface of the proximal side of the supraspinatus muscle and a profile was drawn along the shear wave propagation in the proximal side of the supraspinatus muscle. The ROI were used to measure the mean amplitude value (MAV) of the propagating shear wave in the supraspinatus muscle (supraspinatus-MAV) by using the amplitude images (MRE/Wave, MAYO CLINIC). On the other hand, the profile was used to measure the wavelengths, and the average value (obtained 4 offsets) was recorded. The wavelengths were calculated from half-wavelength that propagated clear wave on the wave image. Assuming that the supraspinatus muscle was linearly elastic, isotropic, homogeneous, and incompressible, the shear modulus (μ), which represented the local elasticity, was calculated using following equation:

$$\mu = \rho f^2 \lambda^2 \quad (1)$$

where ρ is the supraspinatus muscle density ($\fallingdotseq 1$ g/cm^3), f is the frequency and λ is the wavelength.

There are 2 reasons for setting the ROI and profile to the proximal side of the supraspinatus muscle.

The first reason is to evaluate the amplitude and the stiffness in the region of the small attenuation of vibrations. In this method, the vibration pad was placed over the trapezius muscle on the proximal side of the supraspinatus muscle. The vibrations may not propagate sufficiently to the distal side of the supraspinatus muscle because the vibrations attenuate at deeper tissues. The second reason is to evaluate the amplitude and the stiffness in the region that does not include the intramuscular tendon. In the proximal side of the supraspinatus muscle, an influence by the intramuscular tendon may be less because the intramuscular tendon is anatomically located on the distal side of the supraspinatus muscle.

3. Results

Fig. 4 shows the wave images, which were obtained for each readout-angle from 0-150°, from one volunteer. Chroma of the wave images indicates the amplitude of the propagating shear wave in the supraspinatus muscle. In the case of 30-150° readout-angles (Fig. 4b-f), the wave images represented a similar pattern and clear wave propagation especially for near 90° readout-angle in the proximal side of the supraspinatus muscle. In the case of 0° readout-angle (Fig. 4a), the wave images were unclear in the proximal side of the supraspinatus muscle. Moreover, in all readout-angles, the wave was divided into 2 separate waves in the anterior and posterior portions of the supraspinatus muscle, as the wave propagated from the proximal to distal sides of the supraspinatus muscle (Fig. 4g).

Fig. 5 shows the change in mean relative supraspinatus-MAV (n = 7) and the relative perpendicular-MEG-like effect, normalized with those of the 90° readout-angle, as a function of the readout-angle. Both increased when the readout-angle increased between 0° and 90°, and decreased when the readout-angle increased between 90° and 150°. This result showed a correlation between the supraspinatus-MAV and the perpendicular-MEG-like effect. However, the mean relative supraspinatus-MAV in a large readout-angle (120° and 150°) showed a tendency for larger standard deviations compared with those in the small readout-angle (30° and 60°).

Fig. 6 shows wave images obtained for each volunteer in 90° readout-angle. It was found that the direction of the wave propagation with regard to the long axis of the supraspinatus muscle was different for each volunteer.

Fig. 7 shows wave images, which were obtained for each imaging plane, from one volunteer in 90° readout-angle. When the imaging planes were set at the superior portion of the proximal side of the supraspinatus muscle (imaging plane: IP #1 and IP #3), most of the wave images represented clear wave propagation. When the imaging planes were set at the inferior portion of the proximal side of the supraspinatus muscle (IP #2 and IP #4), some wave images represented unclear wave propagation. Thus, supraspinatus muscle stiffness was evaluated in IP #1, because wave images represented clear wave propagation and the supraspinatus muscle was depicted widely. The mean stiffness value of the supraspinatus muscle (n = 7) was 10.6 ± 3.17 (mean ± SD) kPa.

4. Discussion

The purpose of this study was to develop an MRE technique to be applied to the supraspinatus muscle using a conventional MRI. This MRE technique successfully enabled clear wave propagation on the proximal side of the supraspinatus muscle on a condition that the readout-angle was near 90° and the imaging planes were #1 and #3 (superior portion). This paper discusses this condition (the readout-angle and the imaging plane) and this study limitation.

4.1. Readout-angle

In our data, we found that the pattern of the wave images was different in 30-150° and 0° readout-angle on the proximal side of the supraspinatus muscle (Fig. 4). When the readout-angle was 30-150°, there was an arbitrary perpendicular-MEG-like effect. The perpendicular-MEG-like effect sensitizes wave displacements perpendicular to the long axis of the supraspinatus muscle. On the other hand, when the readout-angle was 0°, there was only a parallel-MEG-like effect. The parallel-MEG-like effect sensitizes wave displacements parallel to the long axis of the supraspinatus muscle. In the proximal side of the supraspinatus muscle, it is thus assumed that the wave images in the 30-150° and 0° readout-angle represented wave displacements perpendicular and parallel to the long axis of the supraspinatus muscle, respectively. However, in the case of 30° and 150° readout-angles, the parallel-MEG-like effect was stronger than the perpendicular-MEG-like effect. A possible explanation for this

result is that wave displacements were induced mainly perpendicular to the long axis of the supraspinatus muscle on the proximal side of the supraspinatus muscle. Morphologically, the supraspinatus muscle is one of the uni-circumpennate muscles, in which the muscle fibers are diagonal to the long axis of the muscle. Previous studies have indicated that shear wave displacements were induced primarily perpendicular to the muscle fibers. On the proximal side of the supraspinatus muscle, the fiber orientation is closely parallel to the long axis of the supraspinatus muscle. Therefore, on the proximal side of the supraspinatus muscle, wave displacements might be induced mainly perpendicular to the long axis of the supraspinatus muscle.

It is known that fiber orientation differs between the anterior and posterior portions of the supraspinatus muscle due to the presence of the intramuscular tendon on the distal side of the supraspinatus muscle. In this study, wave images showed a single wave propagation on the proximal side of the supraspinatus muscle. This finding suggests that the anterior and posterior portions of the supraspinatus muscle work as a unit on the proximal side. On the other hand, on the distal side of the supraspinatus muscle, the wave images represented 2 separate wave propagation in the anterior and posterior portions of the supraspinatus muscle, suggesting that the intramuscular tendon between the anterior and posterior portions of the supraspinatus muscle divided the wave propagation. The fiber orientation and the wavelength are simpler on the proximal side compared with that on the distal side of the supraspinatus muscle. Therefore, measuring stiffness might be easier on the proximal side than on the distal side of the supraspinatus muscle.

The study indicated that the supraspinatus-MAV was correlated with the perpendicular-MEG-like effect (Fig. 5). If this correlation is complete, the supraspinatus-MAV should be same in 30° and 150° readout-angle, 60° and 120° readout-angle, respectively. However, in the case of 120° and 150° readout-angles, the mean relative supraspinatus-MAV showed a large standard deviation. Debernard et al. [18] demonstrated that the direction of the wave propagation changed depending on the muscle fibers in MRE. In our data, the direction of the wave propagation to the long axis of the supraspinatus muscle was different for each volunteer (Fig. 6). Therefore, the readout-angle showing the largest supraspinatus-MAV might be different for each individual. If the largest supraspinatus-MAV is not obtained at the 90° readout-angle, the supraspinatus-MAV would be different between the 30° and 150° readout-angle, and between 60° and 120° readout-angle, respectively. The large standard

deviation of the supraspinatus-MAV might be because the muscle fibers direction varies across individuals.

4.2. Imaging planes and stiffness

The supraspinatus muscle is located in the supraspinous fossa. Therefore, the inferior portion of the supraspinatus muscle could be affected by the reflection from the boundaries of the supraspinous fossa compared with that of the superior portion. Accordingly, some wave images might represent unclear wave propagation in the imaging planes #2 and #4 (inferior portion). Alternatively, it may be radically difficult for the wave to propagate in the inferior portion of the supraspinatus muscle because of the muscle architecture. The stiffness value of the supraspinatus muscle also indicated a large standard deviation. Previous studies have demonstrated that the stiffness of skeletal muscles varied based on the pathologic and physiologic states, vibration frequency [14], and fiber orientation [12]. In addition, we did not instruct the volunteers to take body positions, for example, flexing and stretching the elbow joint during imaging. Therefore, the muscle stiffness value may vary even among healthy volunteers.

4.3. Study limitations

First, this study used a small sample size. For evaluating the large variability of the amplitude and the stiffness of the supraspinatus muscle, further studies with larger sample size are required. Second, we could not observe the wave images derived from MEG-like effect perpendicular to the imaging planes. Third, used vibration frequency was only 100 Hz. A higher frequency would provide higher resolution of the stiffness due to a short wavelength. In the 100 Hz vibration, the resolution was sufficient to estimate the stiffness from the overall supraspinatus muscle; however, the resolution was barely sufficient to estimate the stiffness from the proximal supraspinatus muscle. If the stiffness of the supraspinatus muscle is evaluated on the proximal side, a higher frequency may be required to obtain higher resolution of the stiffness.

5. Conclusions

We demonstrated that it is possible to apply MRE to the supraspinatus muscle. Our study findings revealed that wave images showed clear wave propagation on the following conditions: readout-angle was near 90° while the imaging plane was located at the superior portion of the proximal side of the supraspinatus muscle (IP #1 and IP #3). We also recommend that the stiffness of the supraspinatus muscle should be measured at the proximal side.

In addition, MRE with this technique could be one of the routine MRI examinations at the shoulder (T2-weighted image, proton-density-weighted image, etc.) using a clinical shoulder coil. Moreover, a gradient-echo type multi-echo MR sequence can be used in most of the clinical MR imagers. A dedicated MRE sequence (built-in MEG) is not always necessary for MRE. If a wireless synchronization vibration system is used [28,29], MRE of the supraspinatus muscle can be performed by a conventional MRI.

MRE can provide quantitative information on the mechanical properties. This MRE technique could be useful for the diagnosis and for examination of the effect of treatments, such as a tear of the supraspinatus muscle.

Acknowledgments

This work was supported in part by a Grant-in-Aid for Scientific Research (25461838, 26750180) and the Japan Judo Therapist Association.

References

[1] Sandrin L, Tanter M, Gennisson JL, Catheline S, Fink M. Shear elasticity probe for soft tissues with 1-D transient elastography. IEEE Trans Ultrason Ferroelectr Freq Control 2002;49:436-46.

[2] Sarvazyan AP, Rudenko OV, Swanson SD, Fowlkes JB, Emelianov SY. Shear wave elasticity imaging: a new ultrasonic technology of medical diagnostics. Ultrasound Med Biol 1998;24:1419-35.

[3] Muthupillai R, Lomas DJ, Rossman PJ, Greenleaf JF, Manduca A, Ehman RL. Magnetic resonance elastography by direct visualization of propagating acoustic strain waves. Science

1995;269:1854-7.

[4] Mariappan YK, Glaser KJ, Ehman RL. Magnetic resonance elastography: a review. Clin Anat 2010;23:497-511. http://dx.doi.org/10.1002/ca.21006.

[5] Manduca A, Oliphant TE, Dresner MA, Mahowald JL, Kruse SA, Amromin E et al. Magnetic resonance elastography: non-invasive mapping of tissue elasticity. Med Image Anal 2001;5:237-54.

[6] Fattahi N, Arani A, Perry A, Meyer F, Manduca A, Glaser K et al. MR Elastography Demonstrates Increased Brain Stiffness in Normal Pressure Hydrocephalus. AJNR Am J Neuroradiol 2015. http://dx.doi.org/10.3174/ajnr.A4560.

[7] Siegmann KC, Xydeas T, Sinkus R, Kraemer B, Vogel U, Claussen CD. Diagnostic value of MR elastography in addition to contrast-enhanced MR imaging of the breast-initial clinical results. Eur Radiol 2010;20:318-25. http://dx.doi.org/10.1007/s00330-009-1566-4.

[8] Yin M, Glaser KJ, Talwalkar JA, Chen J, Manduca A, Ehman RL. Hepatic MR Elastography: Clinical Performance in a Series of 1377 Consecutive Examinations. Radiology 2016;278:114-24. http://dx.doi.org/10.1148/radiol.2015142141.

[9] Yoshimitsu K, Mitsufuji T, Shinagawa Y, Fujimitsu R, Morita A, Urakawa H et al. MR elastography of the liver at 3.0 T in diagnosing liver fibrosis grades; preliminary clinical experience. Eur Radiol 2015. http://dx.doi.org/10.1007/s00330-015-3863-4.

[10] Li S, Chen M, Wang W, Zhao W, Wang J, Zhao X et al. A feasibility study of MR elastography in the diagnosis of prostate cancer at 3.0T. Acta Radiol 2011;52:354-8. http://dx.doi.org/10.1258/ar.2010.100276.

[11] Sahebjavaher RS, Nir G, Honarvar M, Gagnon LO, Ischia J, Jones EC et al. MR elastography of prostate cancer: quantitative comparison with histopathology and repeatability of methods. NMR Biomed 2015;28:124-39. http://dx.doi.org/10.1002/nbm.3218.

[12] Bensamoun SF, Ringleb SI, Littrell L, Chen Q, Brennan M, Ehman RL et al. Determination of thigh muscle stiffness using magnetic resonance elastography. J Magn Reson Imaging 2006;23:242-7. http://dx.doi.org/10.1002/jmri.20487.

[13] Chakouch MK, Charleux F, Bensamoun SF. Quantifying the Elastic Property of Nine Thigh Muscles Using Magnetic Resonance Elastography. PLoS One 2015;10:e0138873.

http://dx.doi.org/10.1371/journal.pone.0138873.

[14] Hong SH, Hong SJ, Yoon JS, Oh CH, Cha JG, Kim HK et al. Magnetic resonance elastography (MRE) for measurement of muscle stiffness of the shoulder: feasibility with a 3 T MRI system. Acta Radiol 2015. http://dx.doi.org/10.1177/0284185115571987.

[15] Numano T, Mizuhara K, Hata J, Washio T, Homma K. A simple method for MR elastography: a gradient-echo type multi-echo sequence. Magn Reson Imaging 2015;33:31-7. http://dx.doi.org/10.1016/j.mri.2014.10.002.

[16] Basford JR, Jenkyn TR, An KN, Ehman RL, Heers G, Kaufman KR. Evaluation of healthy and diseased muscle with magnetic resonance elastography. Arch Phys Med Rehabil 2002;83:1530-6.

[17] Chen Q, Basford J, An KN. Ability of magnetic resonance elastography to assess taut bands. Clin Biomech (Bristol, Avon) 2008;23:623-9. http://dx.doi.org/10.1016/j.clinbiomech.2007.12.002.

[18] Debernard L, Robert L, Charleux F, Bensamoun SF. Characterization of muscle architecture in children and adults using magnetic resonance elastography and ultrasound techniques. J Biomech 2011;44:397-401. http://dx.doi.org/10.1016/j.jbiomech.2010.10.025.

[19] Green MA, Geng G, Qin E, Sinkus R, Gandevia SC, Bilston LE. Measuring anisotropic muscle stiffness properties using elastography. NMR Biomed 2013;26:1387-94. http://dx.doi.org/10.1002/nbm.2964.

[20] Gennisson JL, Catheline S, Chaffai S, Fink M. Transient elastography in anisotropic medium: application to the measurement of slow and fast shear wave speeds in muscles. J Acoust Soc Am 2003;114:536-41.

[21] Matsuki K, Watanabe A, Ochiai S, Kenmoku T, Ochiai N, Obata T et al. Quantitative evaluation of fatty degeneration of the supraspinatus and infraspinatus muscles using T2 mapping. J Shoulder Elbow Surg 2014;23:636-41. http://dx.doi.org/10.1016/j.jse.2014.01.019.

[22] Hersche O, Gerber C. Passive tension in the supraspinatus musculotendinous unit after long-standing rupture of its tendon: a preliminary report. J Shoulder Elbow Surg 1998;7:393-6.

[23] de Kerviler E, Leroy-Willig A, Jehenson P, Duboc D, Eymard B, Syrota A. Exercise-induced muscle modifications: study of healthy subjects and patients with metabolic myopathies with MR imaging and P-31 spectroscopy. Radiology 1991;181:259-64.

http://dx.doi.org/10.1148/radiology.181.1.1887044.

[24] Fisher MJ, Meyer RA, Adams GR, Foley JM, Potchen EJ. Direct relationship between proton T2 and exercise intensity in skeletal muscle MR images. Invest Radiol 1990;25:480-5.

[25] Shellock FG, Fukunaga T, Mink JH, Edgerton VR. Exertional muscle injury: evaluation of concentric versus eccentric actions with serial MR imaging. Radiology 1991;179:659-64. http://dx.doi.org/10.1148/radiology.179.3.2027970.

[26] Yanagisawa O, Niitsu M, Takahashi H, Itai Y. Magnetic resonance imaging of the rotator cuff muscles after baseball pitching. J Sports Med Phys Fitness 2003;43:493-9.

[27] Rosskopf AB, Ehrmann C, Buck FM, Gerber C, Fluck M, Pfirrmann CW. Quantitative Shear-Wave US Elastography of the Supraspinatus Muscle: Reliability of the Method and Relation to Tendon Integrity and Muscle Quality. Radiology 2016;278:465-74. http://dx.doi.org/10.1148/radiol.2015150908.

[28] Numano T, Kawabata Y, Mizuhara K, Washio T, Hata J, Homma K, editors. A retrofit technology for MR Elastography. Proceedings of the ISMRM 23rd Annual Meeting & Exhibition; 2015 May 30-June 05; Metro Toronto Convention Centre, Canada. Ontario: ISMRM; 2015.

[29] Numano T, Mizuhara K, Kawabata Y, Washio T, Homma K, editors. Magnetic Resonance Elastography with a Wireless Synchronization Pneumatic Vibration System. Proceedings of the Joint Annual Meeting ISMRM-ESMRMB; 2014 May 10-16; Milano Congressi, Italy. Milan: ISMRM; 2014.

Figure Legends

Fig. 1. a: A vibration pad designed using a 3D printer (size, W 5 cm × D 5 cm × H 2.5 cm). b: Position of the vibration pad. c, d: Anterior and posterior views after the vibration pad was fixed on the volunteers.

Fig. 2. Length and direction of green thick arrows indicate the readout gradient intensity (MEG-like effect) and the readout direction (direction of MEG-like effect), respectively. MRE was conducted for

each readout-angle from 0-150° (a). The readout-angle rotation was achieved by rotating the imaging plane (b, c). The green arrows had the same length in each readout-angle because the MEG-like effect was the same. The red solid and blue dashed arrows indicate the perpendicular-MEG-like effect and parallel-MEG-like effect, respectively.

Fig. 3. Two thickest lines of the intramuscular tendon were selected as the baseline on a coronal magnitude image. Imaging planes were set parallel to the baseline, and superior/inferior portion of the proximal side of the supraspinatus muscle.

Fig. 4. a-f: Each image shows magnitude image overlaid with the wave image. Length and direction of green thick arrows indicate MEG-like effect and the direction of MEG-like effect, respectively. The red solid and blue dashed arrows also indicate perpendicular-MEG-like effect and parallel-MEG-like effect, respectively. g: Magnified image of Fig. 5d. In the distal side of the supraspinatus muscle, the wave was divided into two in the anterior and posterior portions (the yellow arrows).

Fig. 5. Mean relative supraspinatus-MAV (normalized with the supraspinatus-MAV of 90° readout-angle) and perpendicular-MEG-like effect (normalized with the perpendicular MEG-like effect of 90° readout-angle). Both increased when the readout-angle increased between 0° and 90°, and decreased when the readout-angle increased between 90° and 150°. *Error bars* show standard deviations.

Fig. 6. Each image shows magnitude image overlaid with the wave image. The white solid and dashed lines indicate the direction of the wave propagation and the long axis direction of the supraspinatus muscle, respectively. Both lines were inscribed in manually.

Fig. 7. a: Magnitude image obtained for each imaging plane (IP #1-4). b: Each image shows magnitude image overlaid with the wave image. c: Representation of wave propagation along the profile on the imaging plane #1 (IP #1).

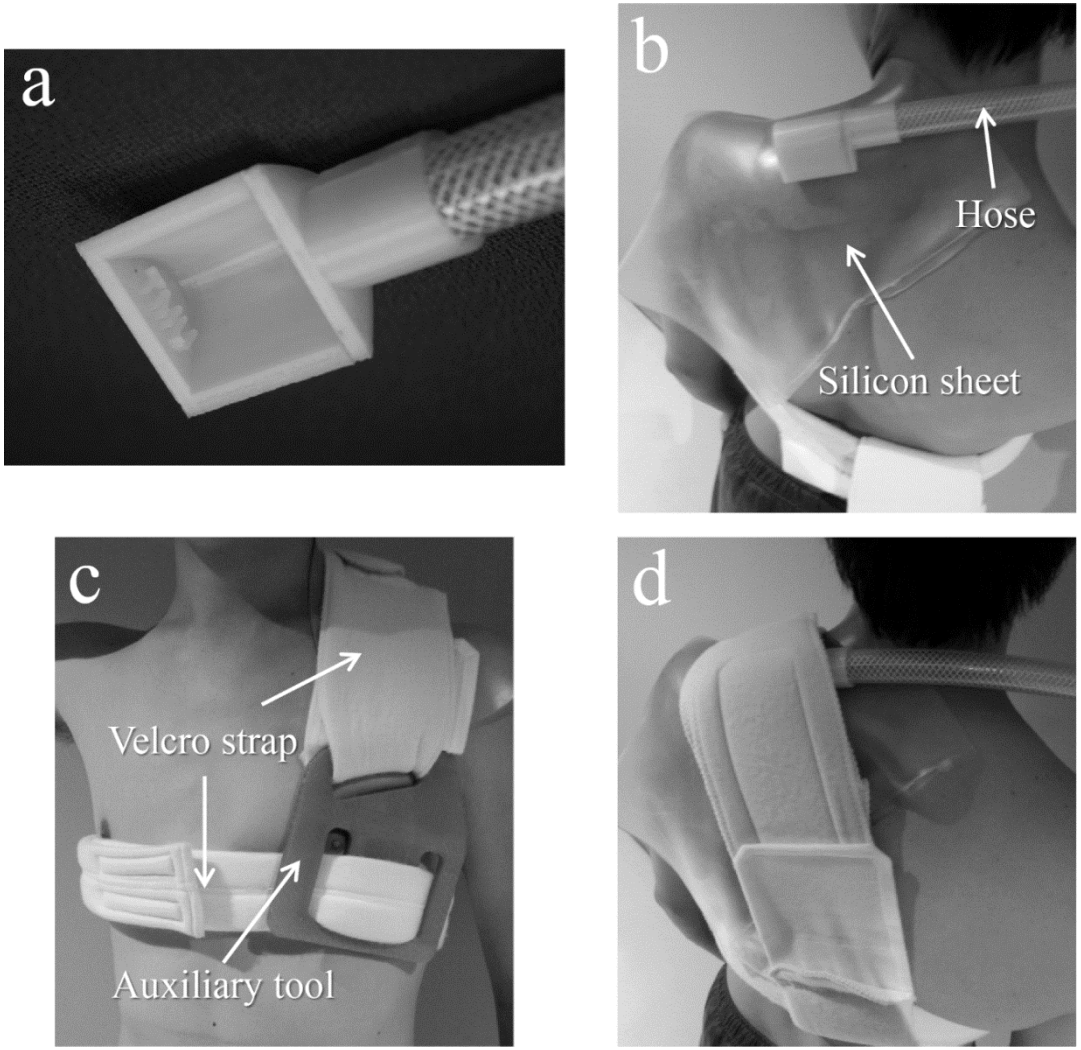

Fig. 1. a: A vibration pad designed using a 3D printer (size, W 5 cm × D 5 cm × H 2.5 cm). b: Position of the vibration pad. c, d: Anterior and posterior views after the vibration pad was fixed on the volunteers.

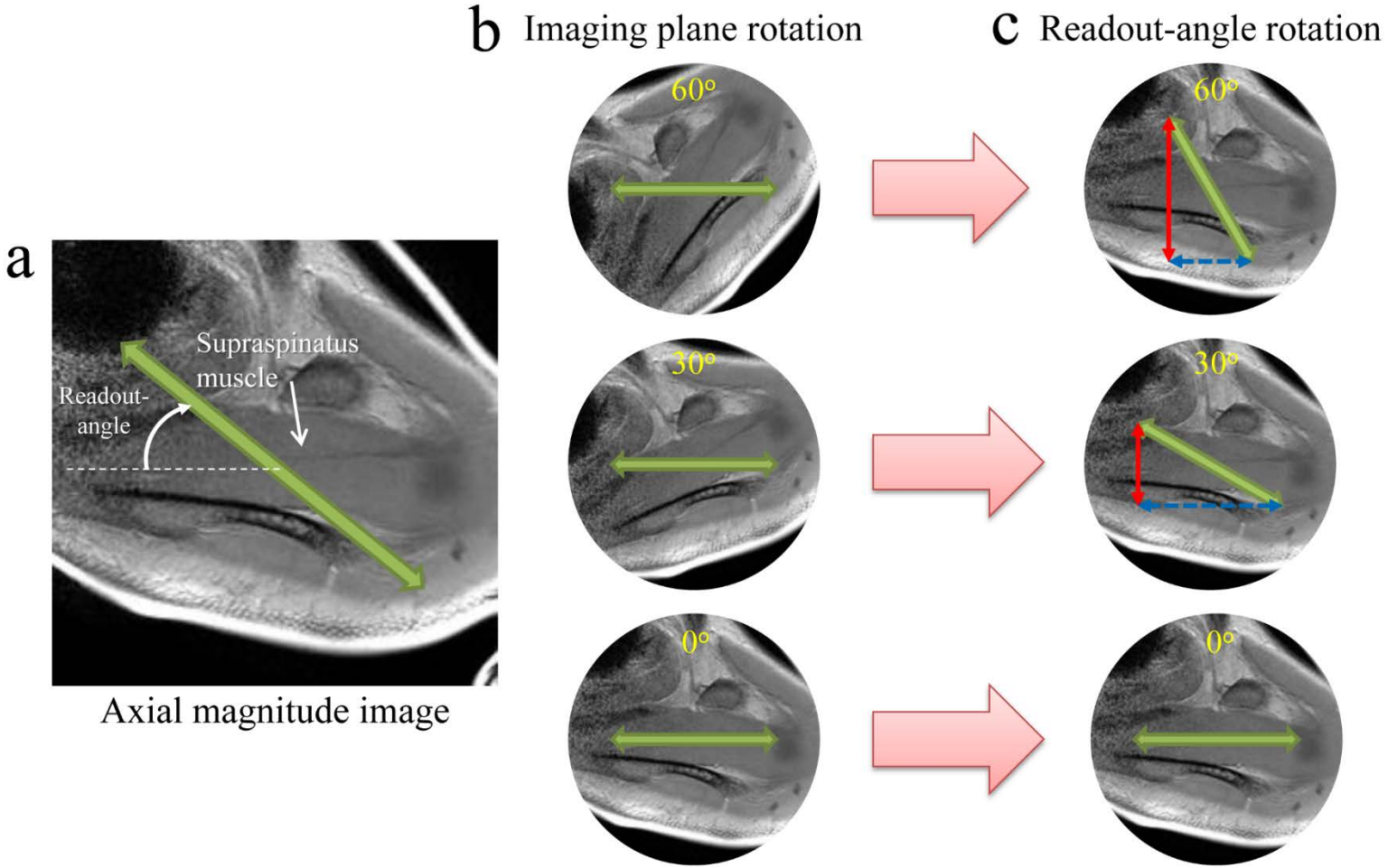

Fig. 2. Length and direction of green thick arrows indicate the readout gradient intensity (MEG-like effect) and the readout direction (direction of MEG-like effect), respectively. MRE was conducted for each readout-angle from 0-150° (a). The readout-angle rotation was achieved by rotating the imaging plane (b, c). The green arrows had the same length in each readout-angle because the MEG-like effect was the same. The red solid and blue dashed arrows indicate the perpendicular-MEG-like effect and parallel-MEG-like effect, respectively.

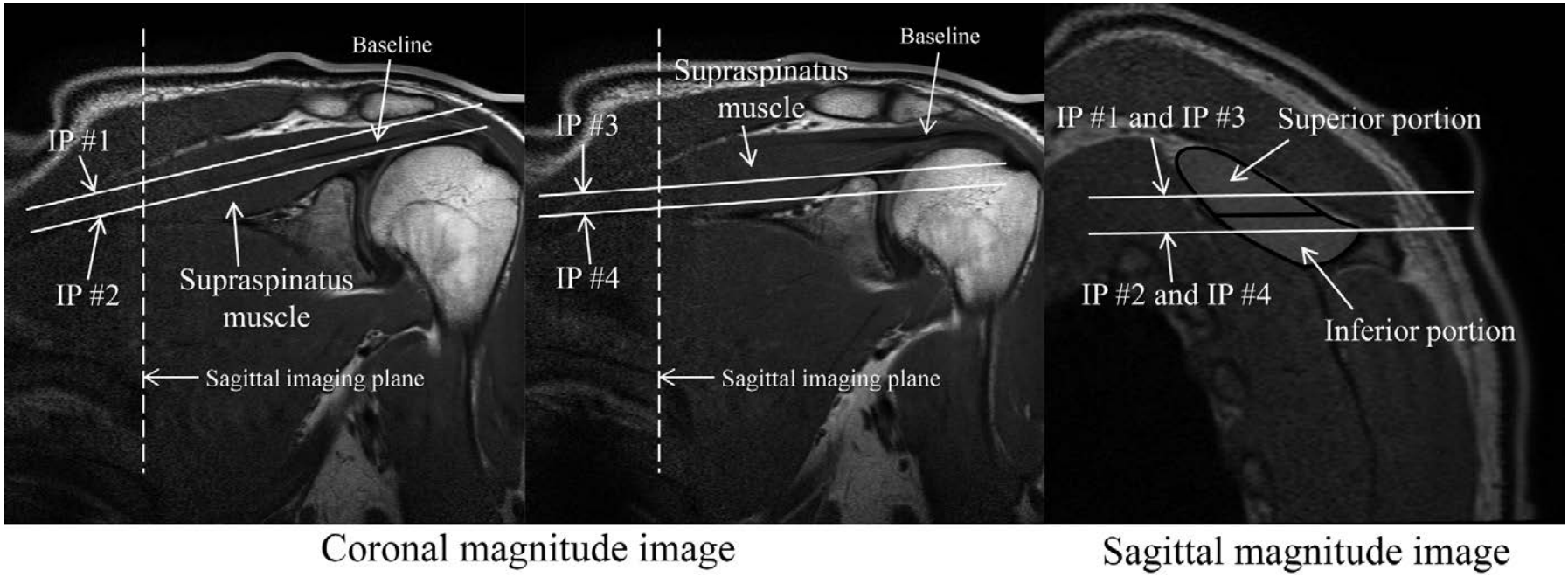

Fig. 3. Two thickest lines of the intramuscular tendon were selected as the baseline on a coronal magnitude image. Imaging planes were set parallel to the baseline, and superior/inferior portion of the proximal side of the supraspinatus muscle.

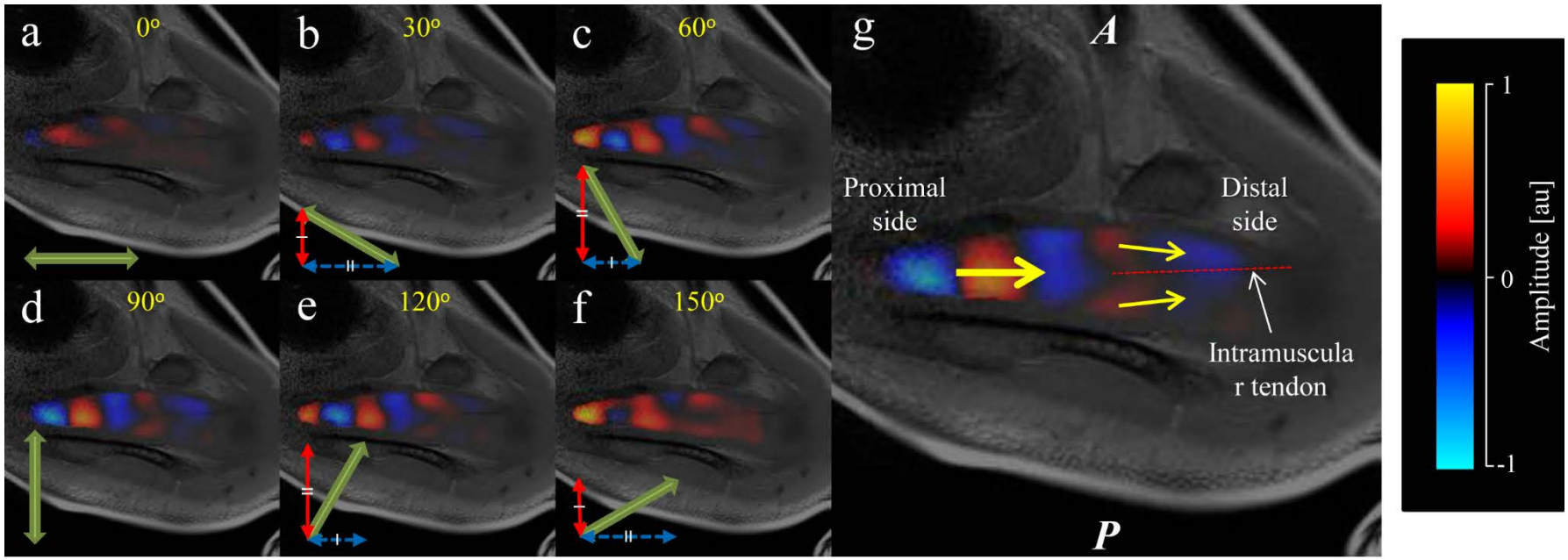

Wave image fusion

Fig. 4. a-f: Each image shows magnitude image overlaid with the wave image. Length and direction of green thick arrows indicate MEG-like effect and the direction of MEG-like effect, respectively. The red solid and blue dashed arrows also indicate perpendicular-MEG-like effect and parallel-MEG-like effect, respectively. g: Magnified image of Fig. 5d. In the distal side of the supraspinatus muscle, the wave was divided into two in the anterior and posterior portions (the yellow arrows).

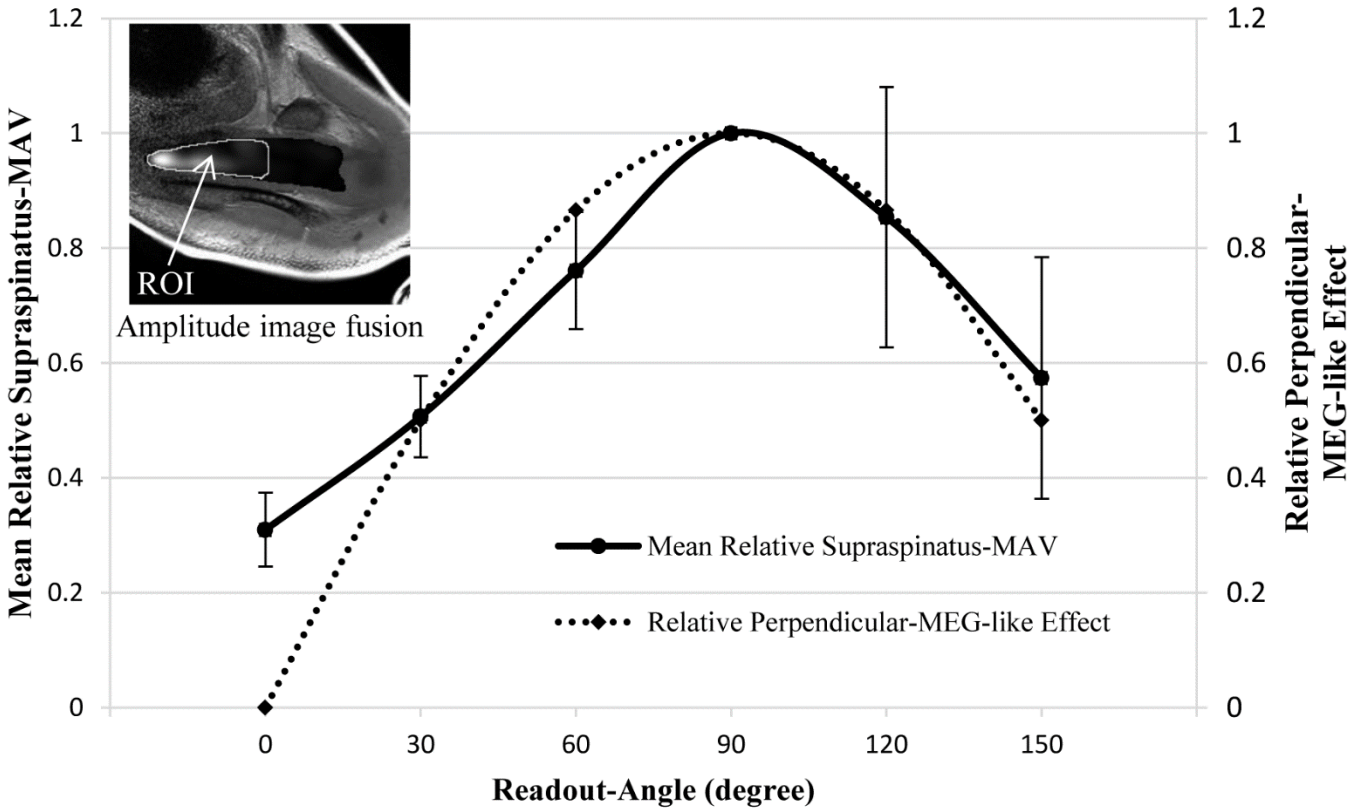

Fig. 5. Mean relative supraspinatus-MAV (normalized with the supraspinatus-MAV of 90˚ readout-angle) and perpendicular-MEG-like effect (normalized with the perpendicular MEG-like effect of 90^{o} readout-angle). Both increased when the readout-angle increased between 0^{o} and 90^{o}, and decreased when the readout-angle increased between 90^{o} and 150^{o}. *Error bars* show standard deviations.

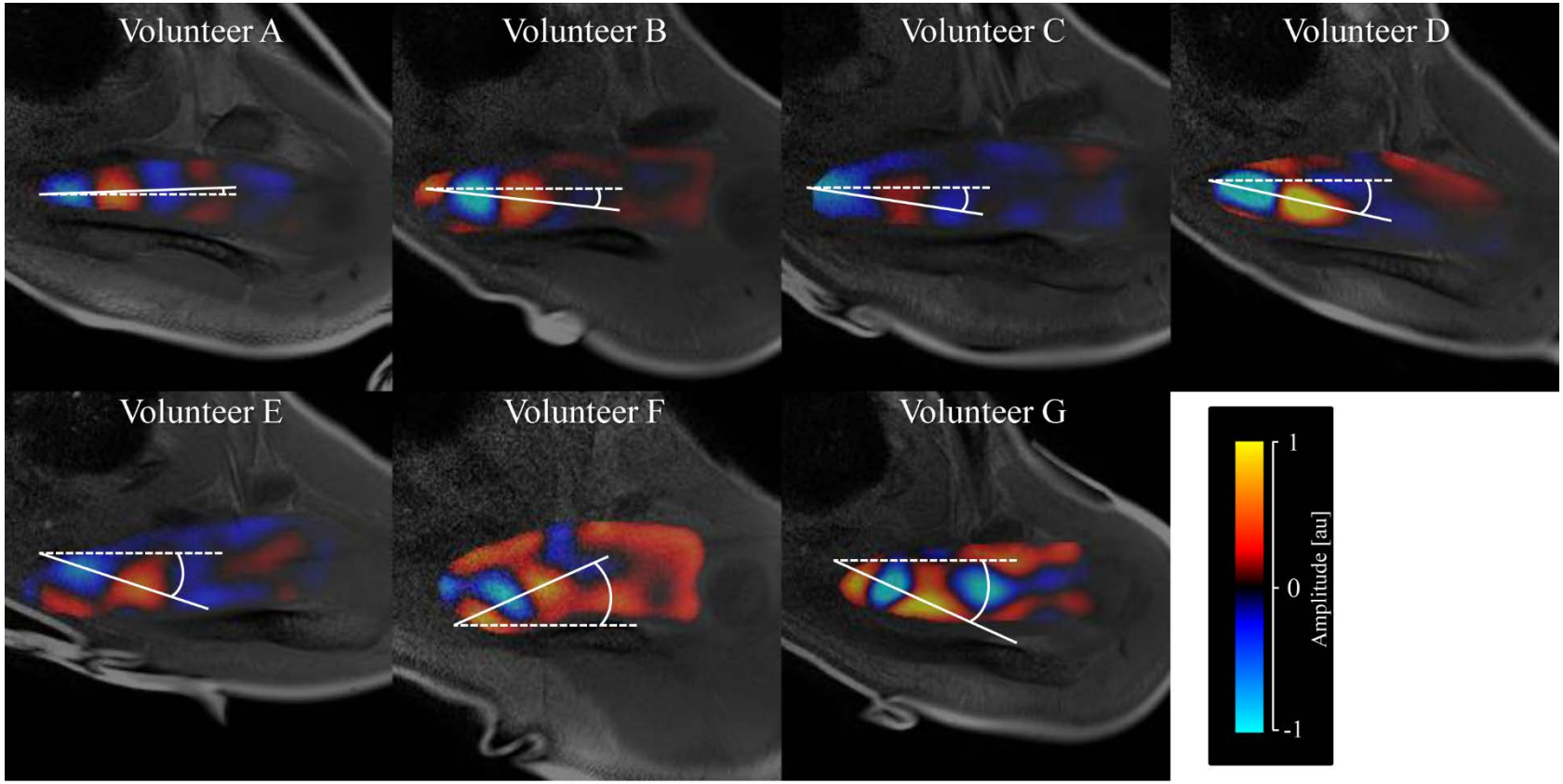

Fig. 6. Each image shows magnitude image overlaid with the wave image. The white solid and dashed lines indicate the direction of the wave propagation and the long axis direction of the supraspinatus muscle, respectively. Both lines were inscribed in manually.

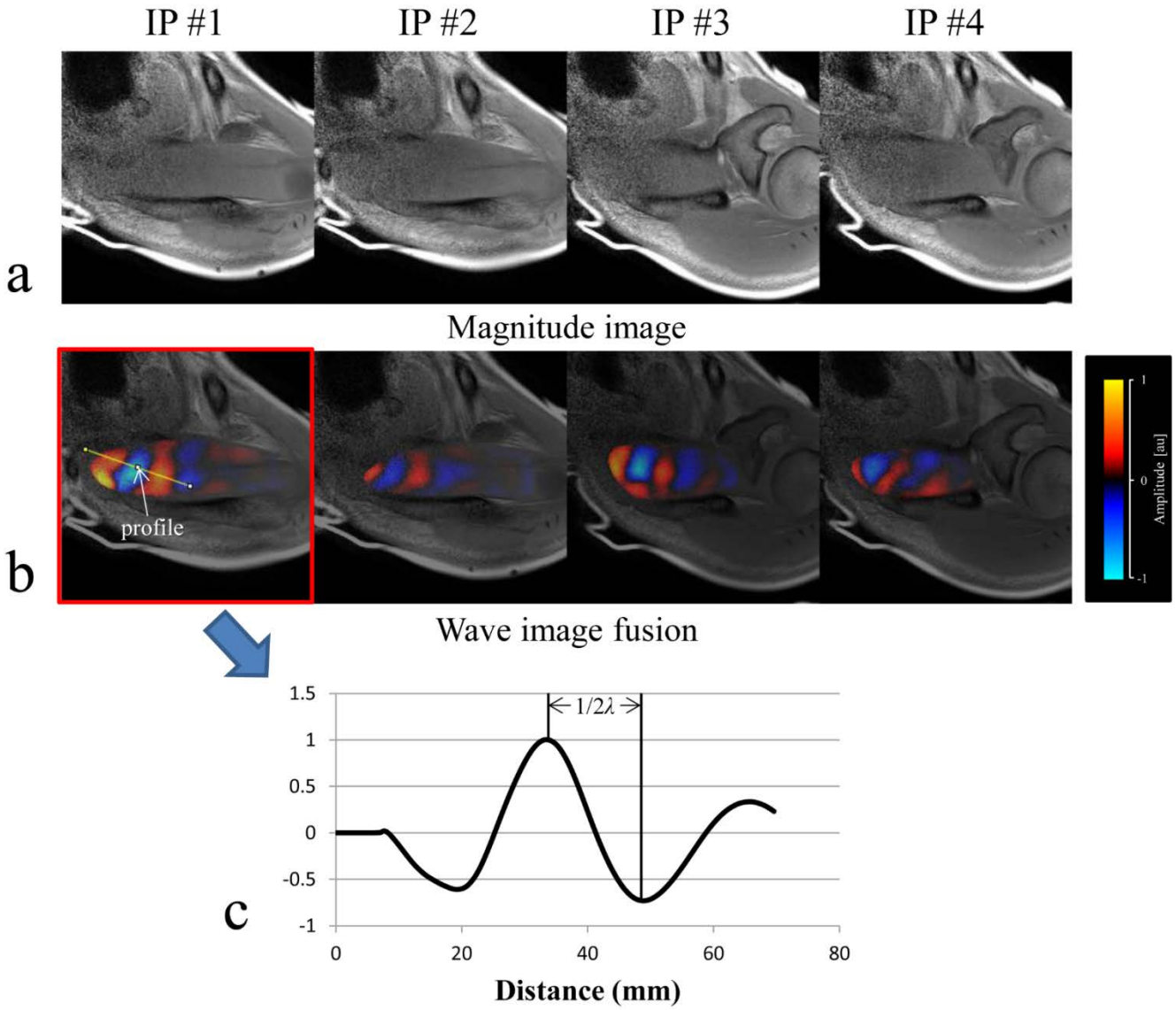

Fig. 7. a: Magnitude image obtained for each imaging plane (IP #1-4). b: Each image shows magnitude image overlaid with the wave image. c: Representation of wave propagation along the profile on the imaging plane #1 (IP #1).